



# Automatic Model Selection Algorithm Based on BYY Harmonic Learning for Mixture of Gaussian Process Functional Regressions Models

Xiaogang Gao, Tang Hui, and Jinye Ma<sup>(✉)</sup>

Department of Mathematics, School of Mathematical Sciences, LMAM, Peking University, Beijing 100871, China  
jwma@math.pku.edu.cn

**Abstract.** Functional mixture model, determining the best functional mixture model based on electi... This article proposes a mixture model of Gaussian process functional regression based on the BYY harmonic learning function (BYY-HLF) method. BYY-HLF has been fully studied in the field of electi... able of Gaussian mixture model (GMM), but it can't be directly used for that of BYY-HLF. We propose the feasible and exacting approach of Gaussian process (GP) model, through which we can find a BYY-HLF model from a GMM. Then, we can make the electi... f... BYY-HLF model. Existing literature has shown that the electi... ed atatic model can be used to fit the data. The electi... featur... e data set.

**Keywords:** Mixture of Gaussian Process Functional Regression Model; Model Selection; Bayesian Ying-Yang Harmonic Learning; Gaussian Process Regression

## 1 Introduction

Gaussian process (GP) model area effect is often based on linear ... a stochastic classification and regression, e.g., classification of handwritten digit and digit recognition and a classification function [1]. However, the current deal with this effect is data effect. Therefore, the Gaussian process function (GPFR) model [2,3] and the exact effect each have been developed to fit their area effect, and fitting their effect, and a data fitting is feasible [4-8].

Like the mixture model, BYY-GPFR model also faces the same problem of the electi... , and the determining the best Gaussian process function (GPFR) model. Since a mixture model of GPFR model will be inevitable, the electi... is great interest. I additi... taking the electi... tility is good and knowledge is extensive, especially in the field of Gaussian process function.

al de ig at atic del electi alg cith . The traditi al eth di t ch e the ti al . be f GPFR c et the gh certai taitical electi citei . F ex. a le, Qia g et al. [6] : edthe litti g ex ectati - axi i ati (SEM) alg cith ba ed the Ba e ia ifc ati citei (BIC)[9]. H e ex, all the ex iti g taitical electi citei a fe ca e a i s ex . be f GPFR c et a d the e fa taitical electi citei i c; a highti ec lexit, i ce ex e edt se eat the h le a a ete eti ai g c ce f c differe t . be f GPFR c et . M c e ex, t chaotic i lati eth d , cha ce ex iblej Mark chai M te C a l [10] a d D richlet c ce e [11], ha e al bee edt deal with the del electi s ble f ix-GPFR del [5, 7, 8]. H e ex, the e eth d ce . i ec llecti galage . be f a le , hich: e lt i a highc tati alc t. F ex Ga ia itce del (GMM), the a t atic del electi alg cith ba ed Ba e ia Yi g-Ya g (BYY) ha lea i g [12, 13] ha e ac ied better ce . lt a d higher c tati need tha th e ba ed taitical electi citeia a d t chaotic i lati eth d [14 20].cdiig a

ba edBed ha lea i g c ix-GPFR de.alBed

8

del ix-GPFR f c aalg cith electi ex e t deledat atic  
ce . lt i

Here, it is the indicated variable is called  $\mathbf{x}$ , and the  $i$ -th  $\mathbf{x}$  is used to indicate the  $i$ -th  $\mathbf{x}$ . For the GMM, we have established the following BYY rule:  $q(z=g) = \pi_g; q(z=g) = \mathcal{N}(\mathbf{z}| \boldsymbol{\mu}_g, \boldsymbol{\Sigma}_g); p(\cdot) = \frac{1}{I} \sum_{i=1}^I \delta(\mathbf{x}_i - \mathbf{z}_i)$ , i.e. the empirical distribution of  $\mathbf{x}$  is

$$p(z=g| \cdot) = \frac{\pi_g \mathcal{N}(\mathbf{z}| \boldsymbol{\mu}_g, \boldsymbol{\Sigma}_g)}{\sum_{s=1}^G \pi_s \mathcal{N}(\mathbf{z}| \boldsymbol{\mu}_s, \boldsymbol{\Sigma}_s)}. \quad (3)$$

Moreover, we give the negative log-likelihood  $r$ , i.e. if  $r = 1$ . Then, we have

$$H(p||q) = J(\Theta) = \frac{1}{I} \sum_{i=1}^I \sum_{g=1}^G \frac{\pi_g \mathcal{N}(\mathbf{x}_i | \boldsymbol{\mu}_g, \boldsymbol{\Sigma}_g)}{\sum_{s=1}^G \pi_s \mathcal{N}(\mathbf{x}_i | \boldsymbol{\mu}_s, \boldsymbol{\Sigma}_s)} \ln (\pi_g \mathcal{N}(\mathbf{x}_i | \boldsymbol{\mu}_g, \boldsymbol{\Sigma}_g)), \quad (4)$$

where  $J(\Theta)$  is called the function of  $\Theta = \{\pi_g, \boldsymbol{\mu}_g, \boldsymbol{\Sigma}_g\}_{g=1}^G$ .

According to BYY learning, the value of  $J(\Theta)$  can be obtained by the following formula [14-20]. Here, we take the empirical distribution of the  $\mathbf{x}$  as the best approximation of  $J(\Theta)$ . If the  $\mathbf{x}$  is the  $i$ -th  $\mathbf{x}$  in  $J(\Theta)$ , the weight of the  $i$ -th  $\mathbf{x}$  is the probability of  $\mathbf{x}_i$  belonging to  $\mathbf{z}$ . Consequently, the  $i$ -th  $\mathbf{x}$  is the  $i$ -th  $\mathbf{x}$  in  $J(\Theta)$ , the weight of the  $i$ -th  $\mathbf{x}$  is the probability of  $\mathbf{x}_i$  belonging to  $\mathbf{z}$ . This is the principle of the BYY learning algorithm based on the empirical distribution of the  $\mathbf{x}$ . The BYY learning has achieved better results than traditional learning methods [14-20].

### 3 Automatic Model Selection Algorithm Based on BYY Harmonic Learning

First, we briefly introduce the  $\mathbf{x}$ -GPFR model. A GP is a collection of random variables, a set of functions which inherit properties of Gaussian distributions [1]. Therefore, if a GP  $\{f(\cdot)\} \in \mathcal{X} \subseteq \mathbb{R}^D$ , we need to determine the empirical function  $m(\cdot)$  and the covariance function  $c(\cdot, \cdot)$ , here.

$$m(\cdot) = \mathbb{E}[f(\cdot)] \text{ and } c(\cdot, \cdot) = \mathbb{E}[(f(\cdot) - m(\cdot))(f(\cdot) - m(\cdot))]. \quad (5)$$

Here, the GP is defined as

$$f(\cdot) \sim \mathcal{GP}(m(\cdot), c(\cdot, \cdot)). \quad (6)$$

The  $\mathbf{x}$ -GPFR model, since  $D = 1$ , we denote the individual variable  $x$ . The  $\mathbf{x}$ -GPFR model with  $G$  GPFR components can be established through the following steps:

$$q(z=g) = \pi_g, \text{ where } \pi_g \geq 0 \text{ and } \sum_{g=1}^G \pi_g = 1; \quad (7)$$

$$q(y(x)|z=g) = \mathcal{GPFR}(x|\mathbf{b}_g, \boldsymbol{\theta}_g, r_g) = \mathcal{GP}\left(m(x|\mathbf{b}_g), c(x, x'|\boldsymbol{\theta}_g) + r_g^{-1} \delta(x, x')\right). \quad (8)$$

In Eq. (8),  $\delta(x, x')$  is the Kullback-Leibler divergence,

$$m(x|\mathbf{b}_g) = \varphi(x)^T \mathbf{b}_g \text{ and } c(x, x'|\boldsymbol{\theta}_g) = \theta_{g0}^2 \exp \left\{ -\frac{(x - x')^2}{2\theta_{g1}^2} \right\}, \quad (9)$$

where  $\varphi(x) = [\varphi_1(x), \varphi_2(x), \dots, \varphi_P(x)]^T$  is a column vector of B-spline basis functions [21] and  $c(x, x'|\boldsymbol{\theta}_g)$  is defined as the squared error function  $\theta_{g0}, \theta_{g1}$ , and  $r_g$  are the parameters.

The Yi-guchi achieves the  $\alpha$ -GPFR model

$$q(z = g, y(x)) = q(z = g)q(y(x)|z = g) = \pi_g \mathcal{GPFR}(x|\mathbf{b}_g, \boldsymbol{\theta}_g, r_g) \quad (10)$$

and it is called the  $\alpha$ -GPFR model.

$$p(z = g, y(x)) = p(y(x))p(z = g|y(x)) = p(y(x)) \frac{\pi_g \mathcal{GPFR}(x|\mathbf{b}_g, \boldsymbol{\theta}_g, r_g)}{\sum_{s=1}^G \pi_s \mathcal{GPFR}(x|\mathbf{b}_s, \boldsymbol{\theta}_s, r_s)}. \quad (11)$$

We denote a training dataset as  $\mathcal{D} = \{\mathcal{C}_i\}_{i=1}^I$ , where  $\mathcal{C}_i = \{(x_{in}, y_{in})\}_{n=1}^{N_i}$  consists of  $N_i$  training samples. It is assumed that  $x_{i1}, \dots, x_{iN_i}$  are  $I$ -dimensional distributed in the interval  $[x_{i1}, x_{iN_i}]$  ( $i = 1, \dots, I$ ). Let  $\mathbf{x}_i = [x_{i1}, \dots, x_{iN_i}]^T$ ,  $\mathbf{y}_i = [y_{i1}, \dots, y_{iN_i}]^T$ , and  $\Theta = \{\pi_g, \mathbf{b}_g, \boldsymbol{\theta}_g, r_g\}_{g=1}^G$ . From the  $\alpha$ -GPFR model,

$$H(p||q) = \sum_{g=1}^G \int p(y(x))p(z = g|y(x)) \ln(q(z = g)q(y(x)|z = g)) dy(x) \quad (12)$$

can be approximated by

$$J(\Theta) = \frac{1}{I} \sum_{i=1}^I \sum_{g=1}^G \frac{\pi_g \mathcal{N}(\mathbf{x}_i|\mathbf{m}_{ig}, \mathbf{C}_{ig})}{\sum_{s=1}^G \pi_s \mathcal{N}(\mathbf{x}_i|\mathbf{m}_{is}, \mathbf{C}_{is})} \ln(\pi_g \mathcal{N}(\mathbf{x}_i|\mathbf{m}_{ig}, \mathbf{C}_{ig})) \quad (13)$$

with  $\mathbf{m}_{ig} = m(\mathbf{x}_i|\mathbf{b}_g)$  and  $\mathbf{C}_{ig} = c(\mathbf{x}_i, \mathbf{x}_i|\boldsymbol{\theta}_g) + r_g^{-1} \mathbf{I}_{N_i}$ , where  $\mathbf{I}_{N_i}$

$\hat{C}_i = \{(x_n, \hat{y}_{in})\}_{n=1}^{N_i}$  if  $\hat{f}_i(x)$  with  $x_n = x_{in} + (n-1)\Delta$ . Doing a fitting, the variance of  $\hat{f}_i(x)$  is

$$\sigma_1^2 = \frac{1}{N_i} \sum_{n=1}^{N_i} (y_{in} - \hat{f}_i(x_{in}))^2. \quad (14)$$

It is clear that

$$\sigma_2^2 = \frac{1}{N_i} \sum_{n=1}^{N_i} (y_{in} - f_i(x_{in}))^2 \quad (15)$$

is a bias estimate of the variance of  $f_i(x)$ . Hence,  $\sigma_1^2$  is a good estimate of the variance that there are significant differences between  $f_i(x)$  and  $\hat{f}_i(x)$ . It is clear,  $\hat{C}_i$  is a good approximation of  $C_i$ . That is to say, the difference between the two coefficients can be validated through experiments in Sect. 4.

Let  $\hat{\mathcal{D}} = [\hat{C}_1, \dots, \hat{C}_I] = [x_1, x_2, \dots, x_N]^T$ , and  $\hat{\mathbf{v}}_i = [\hat{y}_{i1}, \hat{y}_{i2}, \dots, \hat{y}_{iN}]^T$ . It can be regarded as a realization of the following GMM:

$$q(z=g) = \pi_g, \text{ where } \pi_g \geq 0 \text{ and } \sum_{g=1}^G \pi_g = 1; q(\mathbf{v}|z=g) = \mathcal{N}(\mathbf{v}| \mathbf{m}_g, \mathbf{C}_g), \quad (16)$$

$$\text{where } \mathbf{m}_g = m(\mathbf{v}| \mathbf{b}_g) \text{ and } \mathbf{C}_g = c(\mathbf{v}, \mathbf{b}_g) + r_g^{-1} \mathbf{I}_N. \text{ If } Y_i \text{ is achieved, then } q(z=g, \mathbf{v}) = q(z=g) q(\mathbf{v}|z=g) = \pi_g \mathcal{N}(\mathbf{v}| \mathbf{m}_g, \mathbf{C}_g) \quad (17)$$

and it is achieved

$$p(z=g, \mathbf{v}) = p(\mathbf{v}) p(z=g|\mathbf{v}) = p(\mathbf{v}) \frac{\pi_g \mathcal{N}(\mathbf{v}| \mathbf{m}_g, \mathbf{C}_g)}{\sum_{s=1}^G \pi_s \mathcal{N}(\mathbf{v}| \mathbf{m}_s, \mathbf{C}_s)}. \quad (18)$$

The integral calculation of the probability density function of  $\mathbf{v}$  is

$$J(\Theta) = \frac{1}{I} \sum_{i=1}^I \sum_{g=1}^G \frac{\pi_g \mathcal{N}(\mathbf{v}_i | \mathbf{m}_g, \mathbf{C}_g)}{\sum_{s=1}^G \pi_s \mathcal{N}(\mathbf{v}_i | \mathbf{m}_s, \mathbf{C}_s)} \ln (\pi_g \mathcal{N}(\mathbf{v}_i | \mathbf{m}_g, \mathbf{C}_g)). \quad (19)$$

According to the GMM, the aim of  $J(\Theta)$  is to find the total probability of GPFR correctly estimated the best model. Therefore, we can take the model selection criteria to select the best model.

After the training process, we can determine the classification accuracy according to the classification probability, i.e. let

$$z_i = \arg \max_{g \in \{1, 2, \dots, G\}} \frac{\pi_g \mathcal{N}(\mathbf{v}_i | \mathbf{m}_g, \mathbf{C}_g)}{\sum_{s=1}^G \pi_s \mathcal{N}(\mathbf{v}_i | \mathbf{m}_s, \mathbf{C}_s)} (i = 1, 2, \dots, I). \quad (20)$$

The final data of GPFR can be obtained by fitting all training samples. The classification error can be determined by the test set. The classification accuracy is given by the following formula. The detail is referred to [48].

## 4 Experimental Results

In this section, we evaluate the performance of the proposed model and compare it with the effect of different methods on the classification accuracy of the electi alg with. We compare the GPFR model trained using the proposed algorithm with GPFR model,  $\alpha$ -GPFR model, GPFR model, and  $\alpha$ -GPFR model trained by the traditional EM algorithm [2, 3] and the SEM algorithm [6].

Since we are able to compare the prediction ability of the  $\alpha$ -GPFR model, the standard error (RMSE) is chosen as the evaluation metric. It is noted that there are  $T$  test cases in the dataset, and the  $t$ th ( $t = 1, 2, \dots, T$ ) test case is  $y_{t1}, y_{t2}, \dots, y_{tM}$ , which corresponds to the predicted value  $\hat{y}_{t1}, \hat{y}_{t2}, \dots, \hat{y}_{tM}$ , respectively. It follows that

$$\text{RMSE} = \sqrt{\frac{1}{TM} \sum_{t=1}^T \sum_{m=1}^M (y_{tm} - \hat{y}_{tm})^2}. \quad (21)$$

A smaller RMSE indicates a better prediction result.

### 4.1 On Synthetic Datasets

The synthetic data used to train  $S_2, S_3, \dots, S_{10}$  is generated by the following steps: first, each training set consists of 20 training cases and 10 testing cases from a Gaussian distribution. Then, generate the synthetic data and list in Table 1, where  $S_l$  ( $l = 2, 3, \dots, 10$ ) are generated by the  $\alpha$ -GP. Each case consists of 100 features, which are divided into two groups: the first 60 features on the left side feature space and the last 40 features on the right side are divided into two groups.

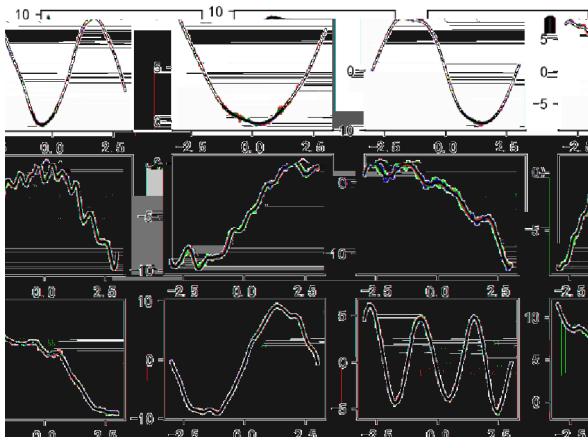
First, we evaluate the effect of the proposed model based on GPFR model. In Fig. 1, we compare the effect of the proposed model with the GPFR model. In Fig. 1(a), we can see that the proposed model has a better effect than the GPFR model. Although there are significant differences between the two models, they both have a similar effect. This indicates that the proposed model is effective.

When using the proposed model, we initialize  $G$  with  $l+3$  features. To illustrate the bad effect of the proposed model, we compare the proposed model with the  $\alpha$ -GPFR model. The proposed model is trained using the EM algorithm [2, 3], which is able to find the best fit for the data. The proposed model is compared with the  $\alpha$ -GPFR model, which is trained using the GPFR algorithm. The proposed model is able to find the best fit for the data, while the  $\alpha$ -GPFR model is not able to do so. This indicates that the proposed model is better than the  $\alpha$ -GPFR model.

From Table 2, we see that the RMSE of the GPFR model and the  $\alpha$ -GPFR model are smaller than that of the GP model and the  $\alpha$ -GP model, which

**Table 1.** Measured function and area under the Gaussian curve generated by the synthetic data set.

Measured function	$\theta^T$	$\sqrt{r^{-1}}$
$x^2$	[0.5, 0.5]	0.15
$(-4(x + 1.5)^2 + 9)1_{\{x < 0\}} + (4(x - 1.5)^2 - 9)1_{\{x \geq 0\}}$	[0.528, 0.4]	0.144
$8 \sin(1.5x - 1)$	[0.556, 0.3]	0.139
$\sin(1.5x) + 2x - 5$	[0.583, 0.2]	0.133
$\sin(4x) - 0.5x^2 - 2x$	[0.611, 0.1]	0.128
$-x^2$	[0.639, 0.1]	0.122
$(4(x + 1.5)^2 - 9)1_{\{x < 0\}} + (-4(x - 1.5)^2 + 9)1_{\{x \geq 0\}}$	[0.667, 0.2]	0.117
$5 \cos(3x + 2)$	[0.694, 0.3]	0.111
$\cos(1.5x) - 2x + 5$	[0.722, 0.4]	0.106
$\cos(4x) + 0.5x^2 + 2x$	[0.75, 0.5]	0.1

**Fig. 1.** The resulting function selected using the synthetic data set. The red, green, blue, and black curves represent the original curve, the selected curve, the true function of the signal curve, and the true function of the selected curve, respectively.

decrease the effectiveness of dealing with the data analysis problem. For B-spline fitting the  $\kappa$ -GP ( $\kappa$ -GPFR) model and the GP (GPFR) model, the need for fitting depends on the type of noise introduced. For the case, we can see that although the effect of GPFR cannot affect the prediction result badly. For  $S_2, S_3, \dots, S_9$ , both the SEM algorithm and the proposed algorithm and the corrected one of GPFR can get a lower RMSE and the higher the number of the SEM algorithm is higher than that of the proposed algorithm. On the other hand,

the SEM algorithm failed to converge at the global minimum for different initial points of GPFR method. On the other hand, it converges to a local minimum faster than the SEM algorithm. In the SEM algorithm, there is a high iteration limit. For  $S_{10}$ , since the SEM algorithm fails to find the global minimum of GPFR method, its RMSE is larger than that of the proposed algorithm.

Taking  $S_9$  for example, we compare the convergence rate of the proposed algorithm with Fig. 2, where different initial points are used. On the left is a diagram of the objective function of the training data set, and on the right is the corresponding convergence curve of the proposed algorithm. It is clear that the proposed algorithm correctly finds all the global minima.

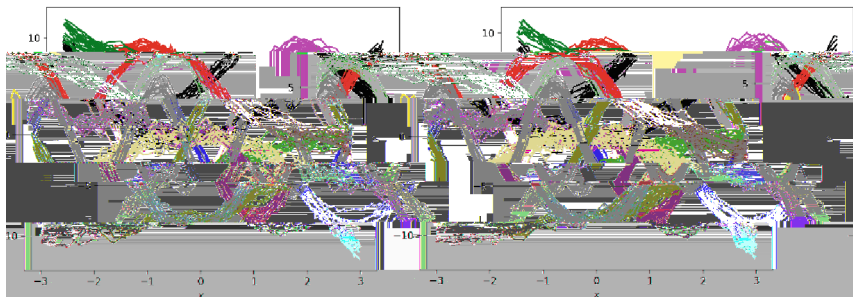
**Table 2.** RMSE and training time for all the methods on the synthetic data set.

	$\mathcal{S}_2$		$\mathcal{S}_3$		$\mathcal{S}_4$	
	RMSE	Time (s)	RMSE	Time (s)	RMSE	Time (s)
GP	5.5831	6.87	4.7878	9.88	4.7798	13.09
$\hat{\alpha}$ -GP (-1)	5.5239	6.12	4.6125	8.90	4.3580	15.84
$\hat{\alpha}$ -GP (+1)	4.8240	7.39	4.6035	17.40	4.3488	23.31
GPFR	5.0759	6.68	4.6864	12.42	4.3051	17.72
$\hat{\alpha}$ -GPFR (-1)	5.0214	8.07	0.9416	15.95	0.9510	18.93
$\hat{\alpha}$ -GPFR (+1)	1.6846	14.20	1.0680	22.66	0.9319	25.79
$\hat{\alpha}$ -GPFR (SEM)	<b>0.4312</b>	20.63	0.4856	41.59	0.5469	58.97
$\hat{\alpha}$ -GPFR (BYY)	0.4401	9.46	<b>0.4746</b>	15.03	<b>0.5403</b>	18.64
	$\mathcal{S}_5$		$\mathcal{S}_6$		$\mathcal{S}_7$	
	RMSE	Time (s)	RMSE	Time (s)	RMSE	Time (s)
GP	4.9213	17.85	4.9897	15.07	5.3096	20.47
$\hat{\alpha}$ -GP (-1)	4.4775	15.03	4.3834	20.14	4.3025	30.66
$\hat{\alpha}$ -GP (+1)	4.5205	28.59	4.3813	29.19	4.3082	30.53
GPFR	4.8079	26.73	4.8649	24.25	4.9871	21.45
$\hat{\alpha}$ -GPFR (-1)	0.8756	31.66	1.0776	29.67	1.3295	32.09
$\hat{\alpha}$ -GPFR (+1)	0.9252	30.58	1.0270	35.37	1.0281	38.44
$\hat{\alpha}$ -GPFR (SEM)	0.5638	81.34	<b>0.6057</b>	87.52	<b>0.6540</b>	92.78
$\hat{\alpha}$ -GPFR (BYY)	<b>0.5573</b>	25.49	0.6137	23.66	0.6571	27.82
	$\mathcal{S}_8$		$\mathcal{S}_9$		$\mathcal{S}_{10}$	
	RMSE	Time (s)	RMSE	Time (s)	RMSE	Time (s)
GP	4.8180	19.67	4.4758	17.82	4.8438	21.67
$\hat{\alpha}$ -GP (-1)	4.4904	24.13	4.1223	32.36	4.5730	32.78

(continued)

**Table 2.** (continued)

	$\mathcal{S}_2$		$\mathcal{S}_3$		$\mathcal{S}_4$	
	RMSE	Ti e ( i )	RMSE	Ti e ( i )	RMSE	Ti e ( i )
$\hat{\pi}$ -GP (+1)	4.4818	23.70	4.1214	30.95	4.5878	28.14
GPFR	4.6871	26.73	4.3686	21.67	4.6865	20.97
$\hat{\pi}$ -GPFR (-1)	1.5325	33.78	1.0585	40.27	1.5279	41.56
$\hat{\pi}$ -GPFR (+1)	1.1891	35.96	0.9789	39.38	1.0343	49.78
$\hat{\pi}$ -GPFR (SEM)	0.6448	99.49	0.6233	116.85	1.4379	130.65
$\hat{\pi}$ -GPFR (BYY)	<b>0.6421</b>	28.91	<b>0.6199</b>	28.62	<b>0.6317</b>	32.46

**Fig. 2.** Clustering result for the electric load data using the electi alg with  $\mathcal{S}_7$  and  $\mathcal{S}_9$ .

## 4.2 On Real-World Datasets

Here, we will use the electric load data introduced by the National Center for Climate Change [8], which record electric load every 15 minutes from 2009 and 2010. Hence, daily electric load can be regarded as a sequence with 96 points. We divide the data into two parts: b-data and a-data, the former including the first 200 training cases and the last 165 testing ones. Moreover, the 56 points in the left side of each day and the 40 points in the right side are used for testing.

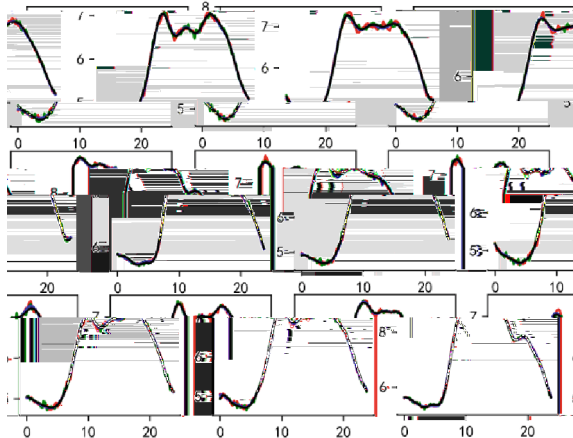


**Fig. 3.** These plots show the electric field data. The red, green, blue, and black curves represent the electric field, the electric field gradient, the electric field derivative, and the electric field derivative squared, respectively. The x-axis is time in seconds, and the y-axis is the electric field in volts per meter.

Although all the cases have the same input, we treat the analysis if the data as the analysis. Like the synthetic data set, we add 1% noise to the  $fR_1$ , which executes correctly and is presented in Fig. 3. A can be seen from the figure, the execution based on GP model is effective for the electric load data set.

Since the best fitting  $\mathcal{R}_1$  and  $\mathcal{R}_2$  are known, we estimate  $G = 3, 6, 9, 12, 15$  from the  $\chi^2$ -GP and  $\chi^2$ -GPFR fitting the EM algorithm. For each fitted algorithm and the SEM algorithm,  $G$  is set to be 15. Beide,  $P_1$  is set to be 30. The exact value is also described in Table 3. For  $\mathcal{R}_1$  and  $\mathcal{R}_2$ , the RMSE for each fitted algorithm is smaller than that of the SEM algorithm since the best fitting gives better results than the traditional one. The clustering result are presented in Fig. 4. On the left a diagram of Fig. 4 are the clustering result for each fitted algorithm using the training data set, respectively. For  $\mathcal{R}_1$  and  $\mathcal{R}_2$ , the best fitting is obtained by the EM algorithm at 13 and 11, respectively. A comparison of Fig. 4, clearly distinguishes different estimation methods. In particular, the clustering result given by the algorithm is more reasonable.

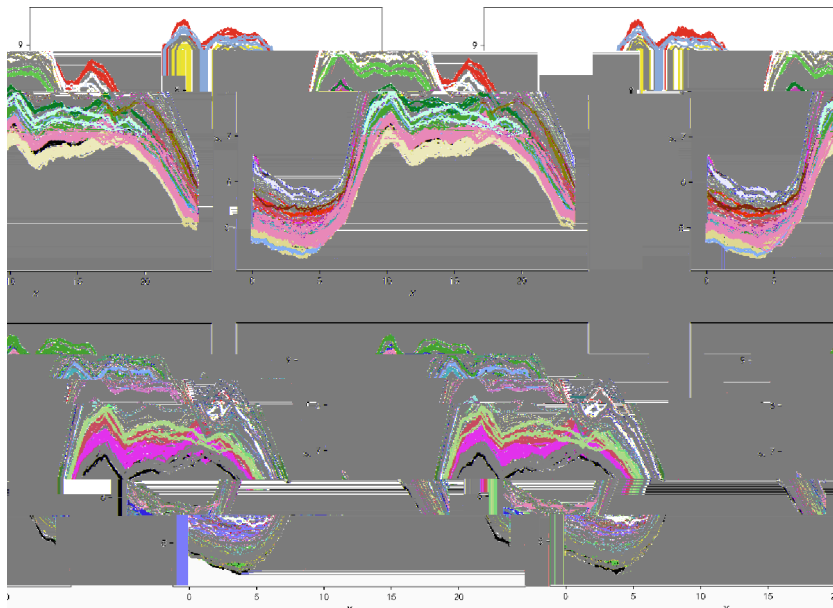


**Fig. 4.** Cl atic g e. li f . c ed a t atic del electi alg with  $\mathcal{R}_1$  a d  $\mathcal{R}_2$ .

**Table 3.** RMSE a d. i gti e f all the eth d  $\mathcal{R}_1$  a d  $\mathcal{R}_2$ .

	$\mathcal{R}_1$		$\mathcal{R}_2$	
	RMSE	Ti e ( i )	RMSE	Ti e ( i )
GP	0.9599	19.43	0.8977	20.39
$\kappa$ -GP (3)	0.9390	20.33	0.8846	21.42
$\kappa$ -GP (6)	0.9387	22.54	0.8854	22.66
$\kappa$ -GP (9)	0.9380	25.99	0.8853	26.09
$\kappa$ -GP (12)	0.9395	29.83	0.8847	31.23
$\kappa$ -GP (15)	0.9401	34.76	0.8872	36.91
GPFR	0.5584	21.30	0.5499	21.59
$\kappa$ -GPFR (3)	0.2089	24.45	0.2133	20.64
$\kappa$ -GPFR (6)	0.1701	25.76	0.1731	24.77
$\kappa$ -GPFR (9)	0.1356	28.93	0.1455	29.45
$\kappa$ -GPFR (12)	0.1248	34.65	0.1314	33.63
$\kappa$ -GPFR (15)	0.1178	35.88	0.1301	36.78
$\kappa$ -GPFR (SEM)	0.1323	150.76	0.1377	170.17
$\kappa$ -GPFR (BYY)	<b>0.1109</b>	33.97	<b>0.1201</b>	34.58

## 5 Conclusion

This paper presents a new method for solving the multi-objective optimization problem based on the BYY hybrid algorithm. The proposed method uses the GPFR model to tackle the non-convexity of the objective function. It also employs a local search strategy to refine the solution. The experimental results show that the proposed method is effective and efficient for solving multi-objective optimization problems. The method can find a set of Pareto-optimal solutions, which provides decision-makers with more choices. The proposed method is compared with other existing methods, such as the SEM algorithm and the PSO algorithm. The results indicate that the proposed method is superior to the other methods in terms of convergence speed and solution quality. The proposed method is also more robust than the other methods, especially for problems with complex constraints. The proposed method is suitable for solving real-world problems, such as engineering design, economics, and management.

**Acknowledgement.** This work was supported by the National Key R & D Program of China (2018AAA0100205).

## References

1. Rawlings, C.E., Williams, C.K.I.: *Galaxy Price Effectiveness Methodology*. MIT Press, Cambridge (2006)
2. Shi, J.Q., Wang, B.: A prediction model for the price of Galaxy. *Statist. Comput.* **18**, 267–283 (2008)
3. Shi, J.Q., Choi, T.: *Galaxy Pricing Regime Analysis*. CRC Press, Boca Raton (2011)
4. Wu, D., Ma, J.: A DAEM algorithm for the price of Galaxy. In: Hwang, D.-S., Ha, K., Han, A. (eds.) ICIC 2016. LNCS (LNAI), vol. 9773, p. 294. Springer, Cham (2016). [https://doi.org/10.1007/978-3-319-42297-8\\_28](https://doi.org/10.1007/978-3-319-42297-8_28)
5. Qiang, Z., Ma, J.: A pricing model for the price of Galaxy. In: Huang, X., Xia, Y., Zhang, Y., Zhang, D. (eds.) ISNN 2015. LNCS, vol. 9377, pp. 335–344. Springer, Cham (2015). [https://doi.org/10.1007/978-3-319-25393-0\\_37](https://doi.org/10.1007/978-3-319-25393-0_37)
6. Qiang, Z., Li, J., Ma, J.: A prediction model for the price of Galaxy. In: 2016 IEEE 13th International Conference on Signal Processing (ICSP), pp. 1089–1094 (2016)
7. Qiang, Z., Ma, J.: A model for the price of Galaxy. In: Shi, Z., Peng, C., Wang, T. (eds.) ICIS 2018. IAICT, vol. 1539, pp. 310–317. Springer, Cham (2018). [https://doi.org/10.1007/978-3-030-01313-4\\_33](https://doi.org/10.1007/978-3-030-01313-4_33)
8. Li, T., Ma, J.: Dirichlet model for the price of Galaxy. *Pattern Recognit.* **134**, 109–129 (2023)
9. Schäfer, G.: Estimating the direct fare model. *Appl. Statist.* **6**(2), 461–464 (1978)
10. Richardson, S., Green, P.J.: On the relationship between the backtracking and the backfitting estimation. *J. Royal Statist. Soc. Ser. B* **59**(4), 731–792 (1997)
11. Ecker, M.D., Wetz, M.: Backward elimination of irrelevant variables. *J. Appl. Statist.* **22**(4), 577–588 (1995)
12. Xu, L.: Ying-Yang machine: A Bayesian -Kullback Leibler divergence learning method. *IEEE Trans. Neural Networks* **12**, 977–988 (1995)
13. Xu, L.: Backtrack, a hybrid RPCL algorithm for the multi-objective optimization problem. *J. Nonlinear Sci.* **11**(1), 43–69 (2001)

14. Che , G., Li, L., Ma, J.: A g adie t BYY ha lea i g alg :ith f c taight li e detec- ti . I : S , F., Zha g, J., Ta , Y., Ca , J., Y , W. (ed .) ISNN 2008. LNCS, l. 5263, . 618 626. S :i ge, Heidelbe g (2008). [ht ://d i .c g/10.1007/978-3-540-87732-5\\_69](http://d i .c g/10.1007/978-3-540-87732-5_69)
15. Li, L., Ma, J.: A BYY cale-i ce e tal EM alg :ith f c Ga ia kt :e lea i g. A l. Math. C . t. **205**(2), 832 840 (2008)
16. Li, L., Ma, J.: A BYY lit-a d- ege EM alg :ith f c Ga ia kt :e lea i g. I : S , F., Zha g, J., Ta , Y., Ca , J., Y , W. (ed .) ISNN 2008. LNCS, l. 5263, . 600 609. S :i ge, Heidelbe g (2008). [ht ://d i .c g/10.1007/978-3-540-87732-5\\_67](http://d i .c g/10.1007/978-3-540-87732-5_67)
17. Ma, J., Wa g, T., X , L.: A g adie t BYY ha lea i g: le Ga ia kt :e v ith a t ated del electi . Ne : c :ti g **56**, 481 487 (2004)
18. Ma, J., Ga , B., Wa g, Y., Che g, Q.: C j. gate a d at :al g adie t: le f c BYY ha lea i g Ga ia kt :e v ith a t ated del electi . I t. J. Patte Rec g . Actif. I tell. **19**(5), 701 713 (2005)
19. Ma, J., Li , J.: The BYY a eali g lea i g alg :ith f c Ga ia kt :e v ith a t ated del electi . Patte Rec g **40**(7), 2029 2037 (2007)
20. Ma, J., He, X.: A fa t. x.ed- i t BYY ha lea i g alg :ith Ga ia kt :e v ith a t ated del electi . Patte Rec g . Lett. **29**(6), 701 711 (2008)
21. B , C.D.: O calc lati g v ith B- li e . J. A : xi ati The c . **6**, 50 62 (1972)